British Journal of Pharmacology (2007) 151, 701–712
 0007–1188/07 $30.00
www.brjpharmacol.org

RESEARCH PAPER

Population pharmacokinetic modelling of non-linear brain distribution of morphine: influence of active saturable influx and P-glycoprotein mediated efflux

D Groenendaal[1,4], J Freijer[2], D de Mik[1], MR Bouw[3], M Danhof[1,2] and ECM de Lange[1]

[1]*Leiden Amsterdam Center for Drug Research, Leiden University, Division of Pharmacology, Leiden, The Netherlands;* [2]*LAP&P Consultants BV, Leiden, The Netherlands;* [3]*GlaxoSmithKline, Clinical Pharmacokinetics Neurology, Harlow, UK*

Background and purpose: Biophase equilibration must be considered to gain insight into the mechanisms underlying the pharmacokinetic-pharmacodynamic (PK-PD) correlations of opioids. The objective was to characterise in a quantitative manner the non-linear distribution kinetics of morphine in brain.
Experimental approach: Male rats received a 10-min infusion of 4 mg kg^{-1} of morphine, combined with a continuous infusion of the P-glycoprotein (Pgp) inhibitor GF120918 or vehicle, or 40 mg kg^{-1} morphine alone. Unbound extracellular fluid (ECF) concentrations obtained by intracerebral microdialysis and total blood concentrations were analysed using a population modelling approach.
Key results: Blood pharmacokinetics of morphine was best described with a three-compartment model and was not influenced by GF120918. Non-linear distribution kinetics in brain ECF was observed with increasing dose. A one compartment distribution model was developed, with separate expressions for passive diffusion, active saturable influx and active efflux by Pgp. The passive diffusion rate constant was 0.0014 min^{-1}. The active efflux rate constant decreased from 0.0195 min^{-1} to 0.0113 min^{-1} in the presence of GF120918. The active influx was insensitive to GF120918 and had a maximum transport (N_{max}/V_{ecf}) of 0.66 ng min^{-1} ml^{-1} and was saturated at low concentrations of morphine ($C_{50} = 9.9$ ng ml^{-1}).
Conclusions and implications: Brain distribution of morphine is determined by three factors: limited passive diffusion; active efflux, reduced by 42% by Pgp inhibition; low capacity active uptake. This implies blood concentration-dependency and sensitivity to drug-drug interactions. These factors should be taken into account in further investigations on PK-PD correlations of morphine.
British Journal of Pharmacology (2007) **151,** 701–712; doi:10.1038/sj.bjp.0707257; published online 30 April 2007

Keywords: morphine; microdialysis; P-glycoprotein; population pharmacokinetic modelling

Abbreviations: BBB, blood–brain barrier; brain ECF, brain extracellular fluid; CBF, cerebral blood flow; Pgp, P-glycoprotein; PK, pharmacokinetics

Introduction

The influence of biophase equilibration must be considered to gain further insight into the mechanisms underlying the pharmacokinetic–pharmacodynamic (PK–PD) correlation of opioid actions in the CNS. In this case, biophase equilibration is mainly determined by blood–brain barrier (BBB) transport. The influence of BBB transport is dependent on three major variables; the morphology and functionality of the brain capillary endothelial cells representing the BBB; the physiochemical properties of the drug; the affinity of the drug for specific transporters present at the BBB. Transport across the BBB can be divided in passive and active transport processes. An important efflux transporter at the BBB is P-glycoprotein (Pgp), which is a member of the adenosine triphosphate-binding cassette superfamily and is encoded by the multidrug resistance gene (MDR1) (Thiebaut *et al*., 1987). This transporter has been shown to have an important influence on the brain distribution of a wide range of drugs (Schinkel *et al*., 1995, 1996; de Lange and Danhof 2002).

It is known that the opioids are substrates for Pgp (Schinkel *et al*., 1995, 1996; Letrent *et al*., 1998, 1999a, b; Henthorn *et al*., 1999; Mahar Doan *et al*., 2002; Wandel *et al*.,

Correspondence: Dr ECM de Lange, Leiden/Amsterdam Center for Drug Research, Leiden University, Division of Pharmacology, PO Box 9502, RA Leiden 2300, The Netherlands.
E-mail: l.lange@lacdr.leidenuniv.nl
[4]Current address: Astellas Pharma Europe BV, Leiderdorp, The Netherlands.
Received 8 September 2006; revised 21 December 2006; accepted 7 March 2007; published online 30 April 2007

2002). Recently, the relative contribution of Pgp-mediated transport and passive permeability on the membrane transport of a wide range of opioids have been studied in an *in vitro* cell system comprising of MDCKII cells transfected with the human Pgp (Groenendaal *et al*., 2007, unpublished results). It was shown that the influence of Pgp on membrane transport is highly dependent on the passive permeability of the opioids. Passive permeability is dependent on physicochemical properties like lipophilicity (van Bree *et al*., 1988); hydrophilic drugs are expected to have a low passive permeability whereas lipophilic drugs often have a high passive permeability. Alfentanil, fentanyl and sufentanil all have affinity for Pgp but the influence of Pgp-mediated transport is minimal because of the high passive permeability rates of these opioids. In contrast, Pgp has a significant influence on the transport of morphine, loperamide and nalbuphine, because their passive permeability is relatively low. For morphine, transcortical microdialysis studies in Pgp-deficient mice (*mdr1a−/−* mice) and wild-type (*mdr1a+/+*) mice have shown that active transport mechanisms influence the brain distribution *in vivo* (Xie *et al*., 1999). In addition, brain perfusion studies have shown that the brain uptake is 1.24 times higher in *mdr1a−/−* mice compared to *mdr1a+/+* mice (Dagenais *et al*., 2004).

Furthermore, PK–PD studies in rats have revealed that, after oral pre-treatment with the specific Pgp inhibitor GF120918, the anti-nociceptive effect of morphine was prolonged due to its prolonged half life in the brain (Letrent *et al*., 1998, 1999a). Bouw *et al*. (2000, 2001) have proposed a compartmental model to account for the delay of the anti-nociceptive effect of morphine relative to corresponding plasma concentrations . It was found that BBB transport accounts for 84% of the observed hysteresis of morphine.

The present investigations focus on the BBB transport of morphine in relation to the effect on the electroencephalogram (EEG) (Groenendaal *et al*., 2007 companion paper). For this purpose, the combined-EEG/microdialysis technique has been developed, which allows simultaneous investigation of both BBB transport and quantitative EEG monitoring in the same rat. The objective of this study was to characterise in a quantitative manner the relative contributions of passive and active transport mechanisms of morphine across the BBB, following intravenous administration of two distinct doses of morphine.

Methods

Study design

To investigate the influence of BBB transport on the PK–PD correlation of the EEG effect of morphine, the study was divided in three separate experiments: (1) EEG experiments, (2) combined EEG/MD experiments and (3) MD experiments. An overview of the experimental groups is shown in Table 1. This paper focuses on the investigation of the transport mechanisms of morphine across the BBB (experiments 2 and 3) on the basis of population PK analysis of blood and extracellular fluid (ECF) concentrations. The PK–PD analysis of the EEG effect of morphine (experiments 1 and 2) will be discussed in a separate paper (Groenendaal *et al*., 2007 companion paper).

Animals

The protocol of these studies was approved by the Committee of Animal Experimentation of the Leiden University. Male Wistar rats weighing between 250 and 350 g (Charles River, Maastricht, The Netherlands) were housed in groups for at least 7 days under standard environmental conditions (temperature 21°C, humidity 60% and 12/12 h dark/light cycle, with lights on at 0700 h). The animals had access to standard laboratory chow (RMH-TM, Hope Farms, Woerden, The Netherlands) and acidified water *ad libitum*. During the experiments, the animals were deprived of food and water.

Surgical procedures

The rats were divided into two different groups, the EEG/MD group ($N=52$) and the MD group ($N=3$). All rats were anesthetized with an intramuscular injection of 0.1 mg kg^{-1} Domitor (1 mg ml^{-1} medetomidine hydrochloride, (Pfizer, Capelle a/d IJssel, The Netherlands)) and a subcutaneous injection of 1 mg kg^{-1} Ketalar (50 mg ml^{-1} Ketamine base, Parke-Davis, Hoofddorp, The Netherlands). Ten days before the start of the experiments, four cortical electrodes were stereotactically implanted into the skull of the EEG rats as described previously (Cox *et al*., 1997). Briefly, the electrodes were placed at the locations 11 mm anterior and 2.5 mm lateral (F_l), 3 mm anterior and 3.5 mm lateral (C_l) and 3 mm posterior and 2.5 mm lateral (O_l) to lambda. A reference

Table 1 Experimental design of the studies investigating the PK–PD relationships of the EEG effects of morphine in rats

Dose (mg kg^{-1})	*Treatment*	*Method*	N	*Body weight (kg)*	*Perfusate concentration (ng ml^{-1})*		
					0	*50*	*500*
4	Vehicle	EEG	7	0.294±0.023	N/A	N/A	N/A
		EEG/MD	14	0.297±0.014	$N=10$	$N=3$	$N=3$
		MD	3	0.304±0.023	$N=3$		
	GF120918	EEG/MD	20	0.300±0.030	$N=10$	$N=5$	$N=5$
10	Vehicle	EEG	7	0.260±0.015	N/A	N/A	N/A
40	Vehicle	EEG	5	0.273±0.026	N/A	N/A	N/A
		EEG/MD	15	0.306±0.019	$N=9$	$N=3$	$N=3$

Abbreviations: EEG,electroencephalogram; MD, multidrug resistance; N/A, not applicable.

electrode was placed on lambda. In addition, a CMA/12 guide cannula with a dummy probe was placed in the striatum of the right brain hemisphere (anterior–posterior: +0.5 mm, lateral: +2.7 mm with bregma as reference and ventral: −3.5 mm ventral to the skull). The MD rats were only instrumented with a CMA/12 guide cannula with a dummy probe. The miniature connector and guide cannula were insulated and fixed to the skull with dental acrylic cement. For drug administration and the collection of blood samples, four indwelling cannulas were implanted in all groups of rats, one in the right femoral artery for collection of serial blood samples and two in the left jugular veins (internal and external) for morphine and midazolam administration. The fourth cannula was implanted into the right femoral vein to administer GF120918 or vehicle and vecuronium bromide. All cannulas were made from pyrogen-free polyethylene tubing (Portex Limited, Hythe, Kent, UK). The arterial cannula consisted of 4 cm (ID = 0.28, OD = 0.61 mm) polyethylene tubing heat-sealed to 18 cm polyethylene tubing (ID = 0.58, OD = 0.96 mm). The venous cannula consisted of 3 cm (ID = 0.28, OD = 0.61 mm) polyethylene tubing heat sealed to 10 cm polyethylene tubing (ID = 0.58, OD = 0.96 mm). The cannulas were subcutaneously tunnelled to the back of the neck of the rats. To prevent clotting the cannulas were filled with a 25% (w/v) polyvinylpyrrolidone (Brocacef, Maarssen, The Netherlands) solution in saline containing 50 IU ml^{-1} heparin (Pharmacy, Leiden University Medical Centre, Leiden, The Netherlands). During the surgical procedures, the body temperature of the rats was maintained constant at 38°C using a CMA/140 temperature controller (Aurora Borealis, Schoonebeek, The Netherlands). After surgery, 4 mg ampicillin (AUV, Cuijk, The Netherlands) was administered to aid recovery. At 16–24 h before the experiments, the dummy microdialysis probe was removed from the microdialysis guide and replaced by the brain probe (CMA/12, 4 mm membrane).

Microdialysis materials

Microdialysis probes, CMA/12 (4 mm, 400 μm ID, 500 μm OD) were supplied by Aurora Borealis Control BV (Schoonebeek, The Netherlands). The probe consisted of a polycarbonate-polyether copolymeric membrane with a molecular cutoff of 20 kDa. The perfusion solution for microdialysis contained (in mM): NaCl 145, KCl 0.6, $MgCl_2$ 1.0, $CaCl_2$ 1.2 and ascorbic acid 0.2 in phosphate buffer, pH 7.4 (Moghaddam and Bunney 1989). The probes were connected to a BAS Beehive infusion pump (Bioanalytical systems Inc., Indiana, IN, USA) with polyethylene tubing (OD 0.61 mm, ID 0.28 mm) supplied by Aurora Borealis Control BV (Schoonebeek, The Netherlands). Before use, the probes were activated according to the manufacturer's protocol (CMA, Sweden).

Microdialysis probe recovery

The microdialysis probe recovery was investigated both *in vitro* and *in vivo*. To check the flow rate through the microdialysis probes, the samples were collected in preweighed collection vials. At the end of the experiment, the vials were weighed to determine the volume collected within the sampling interval and thereby the flow rate. When the flow rate was too low (lower than 95% of 2 μl min^{-1}) or varied too much, the results were omitted from data analysis. The *in vitro* recovery was investigated to check the probe response time to changes in the bulk or perfusate in terms of rate and extent, as well as symmetry (gain = loss). Therefore, the probes were placed in blank perfusion fluid and perfused with blank perfusion fluid for 90 min to stabilize the system. Next, the probes were placed in perfusion fluid containing either 50 or 500 ng ml^{-1} morphine and perfused with blank perfusion fluid for 90 min to determine the gain.

$$\text{recovery} = \frac{C_{\text{out}}}{C_{\text{b}}} \quad (1)$$

where C_{out} represents the morphine concentration in the dialysate outflow, and C_{b} represents the bath concentration in which the probes are placed. After a washout period (blank perfusion fluid in both bath and probe) of 90 min, the probes were placed in blank perfusion fluid and flushed with either 50 or 500 ng ml^{-1} morphine to determine the recovery using the retrodialysis method (Bouw and Hammarlund-Udenaes, 1998). During the experiments, 15 min fractions were collected at a flow rate of 2 μl min^{-1}. The *in vitro* recovery of morphine was calculated by measuring the loss of morphine from the probe into the bath according to equation

$$\text{recovery}_{\textit{in vivo}} = \frac{C_{\text{in}} - C_{\text{out}}}{C_{\text{in}}} \quad (2)$$

where C_{in} is the morphine concentration flushed through the microdialysis probe and C_{out} is the morphine concentration in the dialysate outflow. The recovery was also determined *in vivo* to take into account the influence of periprobe processes (Bungay *et al*., 1990) and was used to calculate ECF concentrations from microdialysate concentrations. The experiment was performed according to a combined retro-DNNF method to determine *in vivo* recovery to obtain concentration- as well as time-dependent recovery values of morphine. The probes were perfused for 60 min with a blank perfusion solution to stabilize the microdialysis and to obtain blank samples. Subsequently, according to a retrodialysis approach (Bouw and Hammarlund-Udenaes, 1998) the microdialysis probes were perfused with morphine concentrations of 0, 50 or 500 ng ml^{-1} (see Table 1) for a period of 60 min before the intravenous administration of morphine, to determine whether the loss of morphine from the probe was concentration dependent or influenced by GF120918. The perfusion concentrations were maintained during the full experiment, according to the DNNF principle (Olson and Justice, 1993), in order to determine time-dependent values for *in vivo* recovery after intravenous (i.v.) administration of morphine. However, in contradiction to previous results for morphine in mice (Xie *et al*., 1999), in this case no conclusions could be drawn from the microdialysis data obtained for the DNNF rats after i.v. administration of morphine. Therefore these data were omitted from further analysis. The *in vivo* recovery was calculated from the retrodialysis period on the basis of the retrodialysis data of the 50 and 500 ng ml^{-1} perfusion concentrations (equation

(2)) and used to correct the microdialysis values obtained from the group of rats with the blank perfusion.

Experimental procedures

The EEG/MD rats were randomly divided in to three groups and received a 10-min intravenous infusion of 4 or 40 mg kg^{-1} morphine, combined with a continuous infusion of the Pgp inhibitor GF120918 or vehicle (Figure 2). The MD rats all received a 10-min infusion of 4 mg kg^{-1} morphine and a continuous infusion of GF120918. Morphine hydrochloride was dissolved in saline. GF120918 infusion consisted of a 1-min bolus infusion of 6 mg kg^{-1} dissolved in dimethyl sulphoxide (DMSO) followed by a continuous infusion of 25 ng min^{-1} dissolved in DMSO/glucose/cyclodextrine 5/5/10% in saline. All rats also received a continuous infusion of midazolam to prevent opioid-induced seizure activity at a rate of 5.5 mg kg^{-1} h^{-1} (Cox *et al*., 1997). Midazolam solutions were prepared in physiological saline containing an equimolar concentration of hydrochloric acid, based on the body weight of the rat. To reach steady-state rapidly, midazolam was administered according to a Wagner infusion scheme, with an initial infusion rate of three times the steady-state infusion rate for 16 min (Wagner 1974).

All experiments started between 0830 and 0930 h to minimize the influences of circadian rhythms. At the start of the experiment ($t=-120$ min), EEG recording was started (when applicable), the microdialysis probes were equilibrated for 60 min and the GF120918 or vehicle infusion was started. After 30 min ($t=-90$ min), midazolam infusion was started followed by the retrodialysis phase of the experiment ($t=-60$ min). Thereafter, at $t=0$ morphine was administered in a zero-order infusion for 10 min using a BAS Beehive infusion pump (Bioanalytical Systems Inc., Indiana, IN, USA). During the experiment, a total number of between 25 and 30 dialysate fractions (10–60 μl each) at a flow rate of 2 μl min^{-1} and 15 arterial blood samples (50–200 μl) were collected at pre-defined time intervals for determination of morphine concentrations. Additionally, six blood samples (50 μl) were collected for determination of GF120918 and midazolam concentrations. The total volume of blood collected did not exceed 2 ml (including blood gas samples, see below). During the experiments, body temperature was stabilized between 37.5 and 38.5°C using a CMA/140 temperature controller (Aurora Borealis, Schoonebeek, The Netherlands). Bipolar EEG leads on the left hemisphere (C_l–O_l) were continuously monitored and analysed offline with fast Fourier transformation. Changes in the amplitudes in the δ-frequency band of the EEG (0.5–4.5 Hz) were used as a pharmacodynamic end point. Details of the EEG measurements will be presented in a separate paper (Groenendaal *et al*., 2007, companion paper).

Monitoring of blood gas status and artificial ventilation

During and after the infusion of morphine, arterial blood samples were collected to monitor arterial pH, pO_2 and pCO_2 levels using a Corning 248 Blood Gas Analyzer (Bayer, Meidrecht, The Netherlands) and to identify respiratory depression. During and after administration of 40 mg kg^{-1} morphine, severe respiratory depression and muscle rigidity occurred. These rats were artificially ventilated with pre-heated air (32°C) using an Amsterdam Infant Ventilator, model MK3 (Hoekloos, Amsterdam, The Netherlands) through a custom made ventilation mask as described by Cox and co-workers (Cox *et al*., 1997). The ventilation settings were ventilation frequency 62 beats min^{-1}, I–E ratio 1:2 and air supply flow rate 0.7–1.0 l min^{-1}. About 5 min after start of the morphine infusion, the rats received an intravenous bolus dose of 0.15 mg vecuronium bromide dissolved in saline and artificial ventilation was started. Vecuronium bromide was used to counteract muscle rigidity to enable artificial ventilation. Vecuronium doses of 0.10 mg were administered repeatedly when muscle rigidity re-appeared until respiratory activity re-occurred. Blood gas status was carefully monitored during and after artificial ventilation.

Drug analysis

Morphine blood samples. Samples were analysed by high-performance liquid chromatography with electrochemical detection (HPLC-ECD) as described previously (Groenendaal *et al*., 2005). Briefly, after addition of internal standard (nalorphine 500 ng ml^{-1}, 50 μl) the blood samples were made alkaline with carbonate buffer (0.15 mM, pH 11, 500 μl) and extracted with 5 ml ethyl acetate. The organic layer was transferred into clean glass tubes and evaporated to dryness under reduced pressure at 37°C. The HPLC system consisted of a LC-10AD HPLC pump (Shimadzu, Kyoto, Japan), a Waters 717 plus autosampler (Waters, Milford, MA, USA), a pulse damper (Antec Leyden, Zoeterwoude, The Netherlands) and a digital electrochemical amperometric detector (DECADE, software version 3.02) from Antec Leyden. The electrochemical detector consisted of a VT-03 electrochemical flow cell combined with a 25 μm spacer and an Ag/AgCl reference electrode operating in the DC mode at a temperature of 30°C, set at a voltage of 0.75 V. Chromatography was performed on C18 Ultrasphere 5 μm column (4.6 mm ID $\times$ 150 mm) (Alltech, Breda, The Netherlands) equipped with a refill guard column. The mobile phase was a mixture of 0.1 M phosphate buffer (pH 4) and methanol (75:25, v/v) and contained a total concentration of 20 mg l^{-1} EDTA and 2.0 mM octane-sulphonic acid. The flow rate was set at 1 ml min^{-1}. Data acquisition and processing was performed using the Empower integration software (Waters, Milford, MA, USA). The intra- and inter-assay variation was less than 10% and the lower limit of quantification was 25 ng ml^{-1} for a 50 μl blood sample.

Morphine dialysate samples. Samples were analysed by HPLC-ECD as described previously (Groenendaal *et al*., 2005). The samples were analysed without sample pre-treatment. Internal standard nalorphine (500 ng ml^{-1}) was added to the samples in a 2:5 ratio, which means 2 μl of internal standard solution for every 5 μl of sample. Since the volume of the microdialysate samples varied throughout the experiment, this method was required to keep the concentration of internal standard constant in all samples. The

HPLC system was the same as described for the blood samples. The electrochemical detector consisted of a VT-03 electrochemical flow cell combined with a 25 μm spacer and an Ag/AgCl reference electrode operating in the DC mode at a temperature of 30°C, set at a voltage of 0.85 V. Chromatography was performed on C18 Ultrasphere 5 μm column (2.0 mm ID × 150 mm) (Alltech, Breda, The Netherlands) equipped with a refill guard column. The mobile phase was a mixture of 0.1 M phosphate buffer (pH 2.5) and methanol (75:25, v/v) and contained a total concentration of 20 mg l^{-1} EDTA and 10 mM octane-sulphonic acid. The flow rate was set at 0.15 ml/min. Data acquisition and processing was performed using the Empower integration software (Waters, Milford, MA, USA). The lower limit of quantification was 0.5 ng ml^{-1} for a 40 μl dialysate sample. The intra-assay variation was less than 0.1% and inter-assay variation was less than 10%.

GF120918 blood samples. Samples were analysed by HPLC with fluorescence detection. After addition of internal standard (chloropromazine, 500 ng ml^{-1}, 50 μl) the samples were treated with sodium hydroxide (0.1 M, 500 μl) and extracted with ethyl acetate. After centrifugation (10 min, 4000 r.p.m.), the organic layer was transferred into clean glass tubes and evaporated to dryness under reduced pressure at 37°C. The HPLC system consisted of a LC-10AD HPLC pump (Shimadzu, Kyoto, Japan), a Waters 717 plus auto sampler (Waters, Milford, MA, USA), and a fluorescence detector (Perkin Elmer) set at $\lambda_{ex} = 260$ nm and $\lambda_{em} = 460$ nm. Chromatography was performed on a stainless steel Microsphere C18 3 μm cartridge column (10 mm × 4.6 mm ID) (Chrompack Nederland BV, Bergen op Zoom, The Netherlands). The mobile phase was a mixture of 0.4 M acetate buffer (pH 4.6) and acetonitrile (50:50, v/v). The flow rate was set at 1 ml min^{-1}. Data acquisition and processing was performed using the Empower integration software (Waters, Milford, MA, USA). The intra- and inter-assay variation was less than 20% and the lower limit of quantification was 100 ng ml^{-1} for a 50 μl blood sample.

Midazolam blood samples. Samples were analysed as described previously by Mandema and co-workers Mandema *et al*. (1991). The method consisted of a liquid–liquid extraction with NaOH and dichloromethane/petroleumether (45:55, v/v). After extraction, samples were injected onto an HPLC coupled to an ultraviolet detector. The intra- and inter-assay variation was less than 6% and the lower limit of quantification was 50 ng ml^{-1} for a 50 μl blood sample.

PK data analysis

The PK data of both blood and brain ECF were analysed using non-linear mixed effect modelling as implemented in the NONMEM software version V, level 1.1 (Beal and Sheiner 1999). Parameter estimation was undertaken using the first-order conditional estimation method (FOCE interaction). All fitting procedures were performed on an IBM-compatible computer (Pentium IV, 1500 MHz) running under Windows XP with the Fortran Compiler Compaq Visual Fortran version 6.1. Structural model selection for both the blood and the ECF PK model was based on the likelihood ratio test, diagnostic plots (observed concentrations vs individual and population predicted concentrations, weighted residuals vs predicted time and concentrations), parameter correlations and precision in parameter estimates. The likelihood ratio test is based on a comparison of the minimum value of the objective function (MVOF) of two models. The significance level was set at 0.01, which corresponds to a decrease of MVOF of 6.6 points when an extra parameter is included in the structural model under the assumption that the difference in MVOF between two nested models is χ^2 distributed. The inter-animal variability in the PK parameters was assumed to be log normally distributed:

$$P_i = P_{typ} \exp(\eta_i) \tag{3}$$

with

$$\eta_i \sim N(0, \omega^2) \tag{4}$$

where P_i is the individual value of the model parameter P, P_{typ} is the typical value (population value) of parameter P in the population, and η_i is realization from a normally distributed inter-animal random variable with mean zero and variance ω^2. Inter-individual variability was investigated for each parameter and was fixed to zero when no significant decrease in the MVOF was obtained. Correlations between the inter-individual variability of the various parameters were graphically explored.

The residual error, which accounts for unexplained errors (e.g. measurement and experimental errors) in the blood drug concentrations, was best described with a proportional error model according to equation

$$C_{obs,ij} = C_{pred,ij} (1 + \varepsilon_{ij}) \tag{5}$$

with

$$\varepsilon_i \sim N(0, \sigma^2) \tag{6}$$

where $C_{obs,ij}$ is the jth observation of the ith individual, $C_{pred,ij}$ is the predicted concentration and ε_{ij} is from a normally distributed residual random variable with mean zero and variance σ^2.

The accuracy of the PK models was investigated by an internal validation method, the visual predictive check (Cox *et al*., 1999; Duffull and Aarons 2000; Yano *et al*., 2001). With this method, 1000 curves were simulated from the final PK parameter estimates. The median, lower (2.5%) and upper (97.5%) limit of the interquantile range of the simulated concentrations were calculated and compared with the position of the observations.

PK analysis of blood profiles

For the development of the PK structural models for blood, both two- and three-compartment models were tested. On the basis of model selection criteria a three-compartment model was chosen. PK analysis was performed with the

PREDPP subroutines ADVAN 11 TRANS 4 implemented in NONMEM with estimation of the PK parameters clearance (Cl), inter-compartmental clearances (Q2 and Q3) and the volumes of distribution (V1, V2 and V3).

To refine the PK model, the relationship between bodyweight and the different parameters was explored graphically. The following equation was used to model the parameter as a function of bodyweight (BW):

$$P_i = \theta_1 \left(1 + \theta_2 \left(BW_i - \text{median}\, BW\right)\right) \tag{7}$$

where P_i is the individual value of a model parameter and θ_1 and θ_2 are the intercept and slope factor of the relationship between the individual parameter and bodyweight.

In addition the influence of co-infusion of GF120918 was also tested with the following the following equation:

$$P_i = \theta_3 \left(1 - GF120918_i\right) + \theta_4 \left(GF120918_i\right) \tag{8}$$

in which GF120918 is a factor, set to 1 if GF120918 is co-infused and set to 0 if vehicle is co-infused.

PK analysis of morphine brain distribution

Simulations were performed to evaluate the influence of different transport mechanisms on the transport of morphine across the BBB. The simulations were performed using Berkeley Madonna (version 8.0.1, Macey & Oyster) and were based on the approach by Hammarlund-Udenaes *et al*. (1997). The population parameter values of the blood PK model were used in the simulations. The non-linear transport model contains specific expressions for (1) passive diffusion, (2) an active saturable uptake mechanism and (3) an active efflux by Pgp (Figure 1). The transport model is based on indications from literature on the active uptake of morphine (Xie *et al*., 1999), simulations of different transport processes (Hammarlund-Udenaes *et al*., 1997) and the models proposed by Upton and co-workers (2000; Xie *et al*., 1999). The model consists of one brain ECF compartment, which is poorly perfused and diffusion-limited. The BBB is located between the blood and ECF compartment.

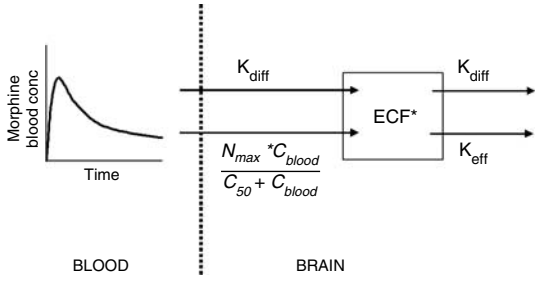

Figure 1 A schematic overview of the non-linear transport model to describe the brain ECF data. The PK of morphine in blood are described with a three-compartment model and used as input function for morphine in the brain. The brain model consists of one brain compartment, and the mass exchange between blood and brain is described with separate expressions for passive diffusion, active saturable influx and active efflux by Pgp, which could be influenced by GF120918. In the figure, k_{diff} is the diffusion rate constant between blood and brain compartment; N_{max} is the maximum active influx, C_{50} is the morphine blood concentration at which 50% of the maximum active influx is reached and k_{eff} is the active efflux rate constant, which is influenced by GF120918.

The mass exchange between the blood and ECF compartment consists of three terms, a passive diffusion flux $Q_{diff}(C_{blood}-C_{ecf})$, an active saturable influx and an active Pgp-mediated efflux, which can be described following equation:

$$\frac{dA_{ecf}}{dt} = -Q_{diff}\left(C_{blood} - C_{ecf}\right) + \frac{N_{max}\, C_{blood}}{C_{50} + C_{blood}} - Q_{eff}\, C_{ecf} \tag{9}$$

in which the right hand side of the equation represents the net mass exchange between the blood and ECF compartment, A_{ecf} is the amount of morphine in the ECF compartment, Q_{diff} is the diffusion clearance, C_{blood} is the concentration in the central blood compartment, C_{ecf} is the concentration in the ECF compartment, N_{max} is the maximal active influx, C_{50} is the morphine concentration in the blood compartment at which 50% of the maximal active influx is reached and ($Q_{eff}C_{ecf}$) is the active efflux by Pgp which is influenced by GF120918.

Accordingly, the concentration in the ECF compartment can be described as

$$\frac{dC_{ecf}}{dt} = \frac{Q_{diff}}{V_{ecf}}\left(C_{blood} - C_{ecf}\right) + \frac{N_{max}}{V_{ecf}}\frac{C_{blood}}{C_{50} + C_{blood}} - \frac{Q_{eff}}{V_{ecf}}\, C_{ecf} \tag{10}$$

Parameter aggregation yields

$$k_{diff} = \frac{Q_{diff}}{V_{ecf}}, \quad N_{max}* = \frac{N_{max}}{V_{ecf}}, \quad k_{eff} = \frac{Q_{eff}}{V_{ecf}} \tag{11}$$

where k_{diff} is the diffusion rate constant and k_{eff} is the active efflux rate constant.

PK analysis of brain ECF profiles

For the development of the PK structural models for brain ECF, the PREDPP subroutine ADVAN6 was used, which is a general nonlinear model that uses the numerical solution of the differential equations. The influence of co-infusion of GF120918 on the PK parameter was investigated following Equation (8).

Chemicals

Morphine hydrochloride was purchased from Pharmachemie (Haarlem, The Netherlands) and GF120918 was kindly provided by GlaxoSmithKline (UK). Midazolam was obtained from BUFA (Uitgeest, The Netherlands). Vecuronium bromide (Norcuron), heparin (20 U/ml) and physiological saline (0.9%) were both obtained from the hospital pharmacy of the Leiden University Medical Center (Leiden, The Netherlands). All chemicals were of analytical grade and solvents were of HPLC grade.

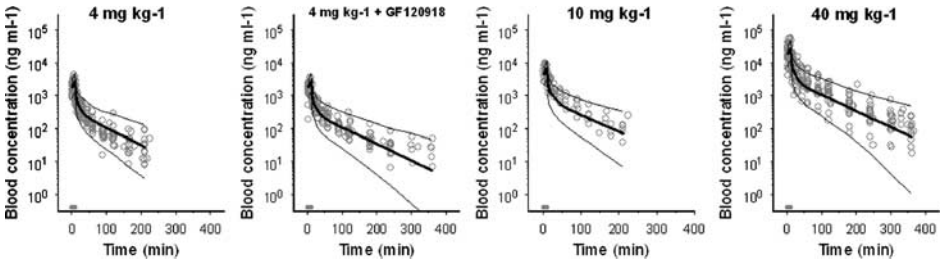

Figure 2 PK of morphine in plasma. Observed (grey dots), population predicted (solid line) and 2.5 and 97.5% quantiles (dotted lines) are depicted for each dose group. The grey bar indicates the infusion time.

Results

PK in blood

Figure 2 shows the observed, population predicted and 2.5 and 97.5% quantiles for morphine concentrations in blood, after administration of a 10-min infusion of 4, 10 and 40 mg kg^{-1} in the presence of vehicle or GF120918. On the basis of MVOF and diagnostics, the PK of morphine in blood was best described with a three-compartment model and was not influenced by co-infusion of GF120918. A tendency towards dose-dependent elimination was observed (Figure 2). The parameters were estimated accurately with acceptable coefficients of variance (Table 2). Covariate analysis showed linear relationships between bodyweight and Cl and between bodyweight and V2. The accuracy of the models was investigated using the predictive check. The selected PK models were good predictors of the time course of morphine after intravenous infusion, as shown by the population prediction and the quantiles (Figure 2).

GF120918 blood concentrations

Three blood samples were collected for determination of the GF120918 concentrations in blood. The first sample was collected at the end of the bolus infusion and the mean (±s.e.m.) concentration in blood was 11 650±2560 ng ml^{-1}. The second and third blood samples were collected randomly from start of the morphine infusion until the end of the experiment. The mean (±s.e.m.) GF120918 concentration in blood was 214±16 ng ml^{-1}, which was sufficient to block Pgp (GSK, personal communication).

Midazolam blood concentrations

Three blood samples were collected for determination of the midazolam concentrations in blood. The first sample was collected before morphine administration and the mean (±s.e.m.) concentration in blood was 879±75 ng ml^{-1}. The second and third blood samples were collected randomly from the start of the morphine infusion until the end of the experiment. The mean (±s.e.m.) midazolam concentration in blood was 937±56 ng ml^{-1}, which was sufficient to suppress potential opioid-induced seizure activity (Cox *et al*., 1997).

Table 2 Population pharmacokinetic parameter estimates of morphine in blood obtained with a three-compartment model

Parameter	*Estimate*	*CV%*	*LLCI–ULCI*
Structural model			
Cl (ml min^{-1})			
Intercept	20.0	5.6	18.5–23.1
Slope factor	5.35	25.2	5.66–11.3
V1 (ml)	68.1	16.7	45.8–90.4
Q2 (ml min^{-1})	15.5	11.3	12.1–18.9
V2 *(ml)*			
Intercept	739	7.6	629–849
Slope factor	8.50	17.1	2.70–7.99
Q3 (ml min^{-1})	17.8	18.4	11.4–24.2
V3 (ml)	133	15.9	91.6–174
Interanimal variability			
ω^2 Cl	0.129	17.2	0.085–0.173
ω^2 *V2*	0.099	24.7	0.051–0.147
Residual variability			
Proportional error	0.074	10.2	0.059–0.089

Abbreviations: Cl, clearance; CV%, coefficient of variation; LLCI, lower limit of confidence interval; Q2/Q3, inter-compartmental clearances; slope factor, linear relationship between body weight and Cl or V2; ULCI, upper limit of confidence interval; V1, volume of distribution in central compartment; *V2/V3*, volumes of distribution in peripheral compartment.

Recovery of the microdialysis probes

The *in vitro* recovery experiments showed that gain is equal to loss, indicating that no adhesion to probe materials occurs with an instantaneous reflection of bulk morphine concentrations. The individual recovery values were calculated on the basis of six microdialysis fractions. The average recovery values *in vitro* were 25±5.0 and 24±5.6% for retrodialysis solutions of 50 and 500 ng ml^{-1} morphine, respectively.

The average recovery values *in vivo,* as determined, before systemic administration of morphine, were 16±9.9 and 20±3.5% for retrodialysis solutions of 65 and 622 ng ml^{-1} morphine. No difference was found between the vehicle and GF120918 pretreated group, indicating that co-infusion of GF120918 does not influence the *in vivo* recovery. Since the experimental design does not allow estimation of individual recovery values, for the 4 mg kg^{-1} morphine and the 4 mg kg^{-1} + GF120918 group the average recovery value of 16.1% was used and for the 40 mg kg^{-1} morphine group, a value of 20.3% was used.

PK in brain ECF

Morphine brain distribution kinetics was investigated using two distinctly different doses for an extensive period of 4–6 h. With this approach, data were collected over a broad concentration range, which allowed detailed PK analysis. The individual observed morphine concentrations in brain ECF are shown in Figure 3. The brain ECF concentrations increased rapidly after start of the morphine infusion, the maximum concentration of morphine was observed within 40 min after start of the infusion for the $4\,mg\,kg^{-1}$ groups and within 20 min for the $40\,mg\,kg^{-1}$ group. For the $4\,mg\,kg^{-1}$ groups, after 20 min a relatively stable plateau in morphine brain ECF concentrations was reached. However, with the $40\,mg\,kg^{-1}$ dose, a clear decline in brain ECF concentration was observed. When morphine concentrations were normalized to a dose of $4\,mg\,kg^{-1}$, the non-linearity in distribution kinetics in brain ECF was evident (Figure 4). Moreover, at higher doses a reduction of the dose-normalized area under the curve (AUC) is observed. The dose-normalized AUC was calculated over the largest common interval (0–165 min) using the log-linear trapezoidal rule and had mean values of 6810 ± 1890, 8460 ± 2790 and $3990 \pm 2180\,ng\,h\,ml^{-1}$ for the $4\,mg\,kg^{-1}$, $4\,mg\,kg^{-1}$ + GF120918 and the $40\,mg\,kg^{-1}$ morphine group, respectively.

For the $4\,mg\,kg^{-1}$ dose group, the net elimination from the brain was much slower compared to the $40\,mg\,kg^{-1}$ dose group. This process could not be described with a linear brain model, and the profiles suggested that transport of morphine is influenced both by an active influx transport process and the active efflux transport, mediated by Pgp. The active influx was supposed to be saturated at the lower concentrations of morphine ($4\,mg\,kg^{-1}$).

This behaviour of the proposed brain distribution model was evaluated using simulations in Berkeley Madonna.

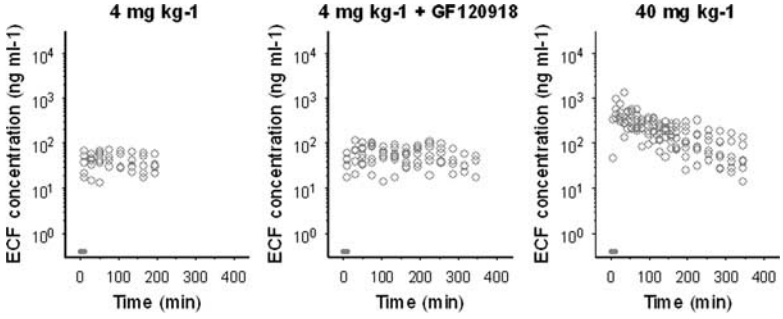

Figure 3 Observed morphine brain ECF concentrations for each dose group. The grey bar indicates the infusion time.

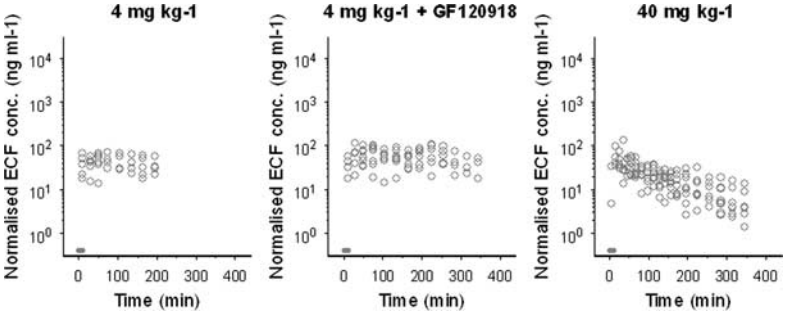

Figure 4 Observed morphine brain ECF concentrations after normalization for dose (normalization dose $4\,mg\,kg^{-1}$). The grey bar indicates the infusion time. The dose is depicted at the top of each panel.

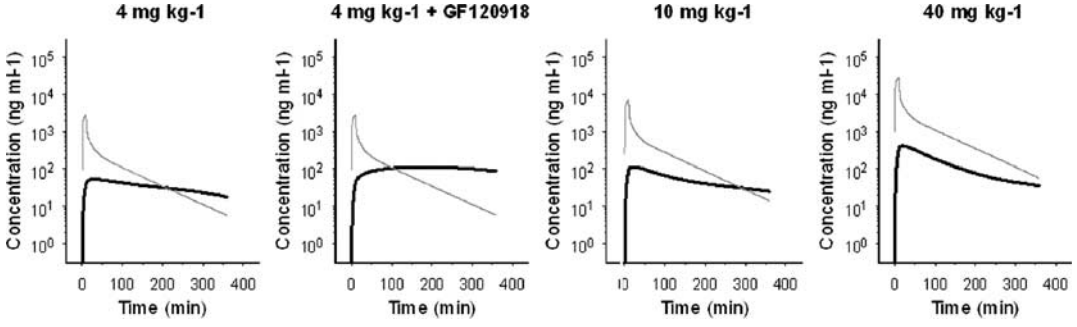

Figure 5 Simulations of the proposed non-linear transport model, consisting of separate expressions for passive diffusion, active saturable influx and active efflux by Pgp, which could be influenced by GF120918. The grey line represents the PK in plasma and the black lines the PK in brain ECF.

Figure 5 shows the simulated time courses of the brain ECF concentrations upon administration of morphine with doses ranging from 4 to 40 mg kg^{-1} in the absence and presence of GF120918. Results show that, consistent with the observations in the experiments, relatively stable 'plateau' brain ECF concentrations or morphine are observed at low doses, while with increasing doses a clear decline is observed. Next, the non-linear transport model was fitted to the data and resulted in a good description of the brain ECF profiles. Morphine concentrations could be adequately described with this model as shown in Figure 6 and Table 3. Specifically, when the active efflux of morphine in the presence of GF120918 was set to zero, this resulted in a significant worsening of the fit. The best fit was obtained when different values of the efflux rate constant k_{eff} were estimated for the presence or absence of GF120918. In the presence of GF120918, the value of the efflux rate constant k_{eff} decreased by about 40%. This suggests that around 50% of the active efflux process is mediated by, transporters other than Pgp.

In the population analysis, precise estimates could be obtained for all parameters. The coefficients of variation were all below 50% except for the C_{50} estimate. Inter-animal variability (ω^2) was also estimated for k_{diff} and k_{eff}. In addition, a correlation was found between the *post hoc* individual estimates of k_{diff} and k_{eff} and therefore a covariance block was included in the final model. Inter-animal variability could not be estimated accurately for the other parameters and was therefore fixed to zero. The individually observed morphine brain ECF concentrations do not deviate substantially from individual predicted concentrations, as is shown by the goodness-of-fit plots (Figure 7). The weighted residuals, which is the difference between observed and predicted morphine ECF concentrations, were randomly distributed around zero in time, indicating that the structural model is plausible. In general, the model can predict the brain ECF concentration adequately as is shown in Figures 6 and 7. The model development was mainly driven by knowledge of different transport processes, such as efflux by Pgp (Xie *et al*., 1999; Letrent *et al*., 1999a, b).

Discussion

The influence of biophase equilibration must be assessed considered to gain a better understanding of the mechanisms underlying the PK–PD correlation of the central effects of the opioids. Biophase equilibration in this example is mainly determined by BBB transport. For morphine, there are clear indications that BBB transport influences the

Table 3 Population pharmacokinetic parameter estimates of the non-linear transport model of morphine in brain ECF

Parameter	*Estimate*	*CV%*	*LLCI–ULCI*
Structural model			
k_{diff} (min^{-1})	0.0014	12.6	0.0010–0.0017
k_{eff} (min^{-1})			
−GF120918	0.0195	12.2	0.0149–0.0241
+GF120918	0.0113	25.4	0.0057–0.0169
N^*_{max} (ng min^{-1})	0.658	26.1	0.321–0.995
C_{50} (ng ml^{-1})	9.92	71.5	−3.97–23.8
Interanimal variability			
$\omega^2 k_{diff}$	0.238	56.3	−0.025–0.501
$\omega^2 k_{eff}$	0.080	36.8	0.022–0.137
$\omega^2 k_{eff} \sim \omega^2 k_{eff}$	0.059	85.0	−0.039–0.158
Residual variability			
Proportional error	0.094	21.4	0.055–0.134

Abbreviations: C_{50}, morphine blood concentration at which 50% of the maximal active influx is reached; CV%, coefficient of variation; k_{diff}, diffusion rate constant; ECF, extracellular fluid; k_{eff}, active efflux rate constant; LLCI, lower limit of confidence interval; N^*_{max}, maximum active influx; ULCI, upper limit of confidence interval.

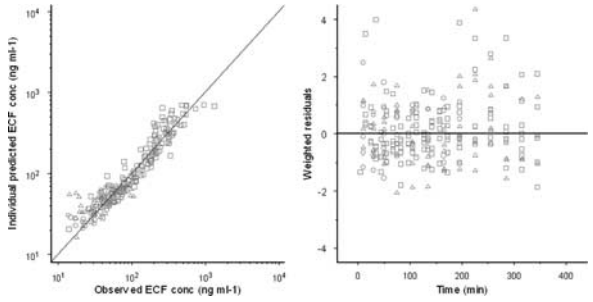

Figure 7 Goodness-of-fit plots of morphine concentrations in brain ECF for the non-linear transport model. In the left panel, a scatterplot shows the observed morphine concentrations versus the individual model predictions. The line represents the line of unity. In the right panel, the scatterplot shows weighted residuals versus time. The circles represent the data of the 4 mg kg^{-1} morphine group, the triangles represent the 4 mg kg^{-1} +GF120918 group and the squares represent the 40 mg kg^{-1} morphine group.

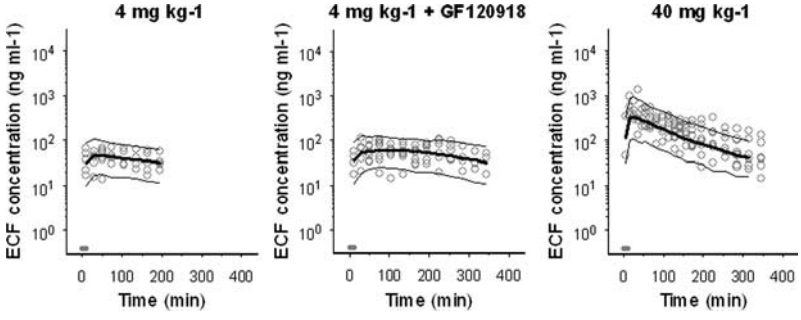

Figure 6 PK of morphine in brain ECF. Observed (grey dots), population predicted (solid line) and 2.5 and 97.5% quantiles (dotted lines) are depicted for each dose group. The grey bar indicates the infusion time.

biophase equilibration (Bouw *et al*., 2000). As part of the present investigations that focus on the BBB transport of morphine in relation to the PK–PD correlation for the effect on the EEG (Groenendaal *et al*., 2007 companion paper), the objective of the present study was to characterize, in a quantitative manner, the influence of passive and active transport mechanisms of morphine across the BBB. To this end, a wide range of morphine concentrations in blood and brain ECF following intravenous administration of 4 mg kg^{-1} morphine, in the presence and absence of GF120918, and 40 mg kg^{-1} morphine alone have been analysed on the basis of a three compartment PK model and a one-compartment brain distribution model, respectively. It was deduced that BBB transport of morphine consists of passive diffusion, in parallel with active saturable influx and active efflux mechanisms.

PK in blood

The PK of morphine in blood was best described by a three-compartment model, based on blood concentration data up to 360 min after the start of the morphine infusion. In previous studies, plasma PK were described with a two-compartment model, for data up to 180 min (Bouw *et al*., 2000; Tunblad *et al*., 2004). This longer sampling period allows a more detailed analysis of the terminal phase of the morphine PK, especially following the administration of a higher dose (40 mg kg^{-1}). A tendency towards dose-dependent elimination was observed (Figure 2). However, there are no indications from literature for a dose-dependent elimination of morphine, nor could it be identified on the basis of the current data.

It is known that morphine is metabolized into glucuronides. The main metabolite in rats is morphine-3-glucuronide (M3G). In humans, morphine is also metabolized into M6G. However, upon intravenous administration of morphine in rats, M6G has not been detected in plasma (Coughtrie *et al*., 1989; Salem and Hope, 1997; van Crugten *et al*., 1997). Research has shown that M3G only has minor antinociceptive effects (Ekblom *et al*., 1993; Gardmark *et al*., 1993), it has not been analysed in this study. Also, because M3G is not a Pgp substrate (Xie *et al*., 1999; Letrent *et al*., 1999a), the potential influence of M3G on Pgp interaction could be excluded. On that basis it seems highly unlikely that the glucuronide metabolites are of significant influence on the BBB transport in our experiments.

Distribution into brain ECF

The proposed novel brain distribution model is rather complex; in contrast to previously proposed models it contains a passive diffusion component and two active transport mechanisms, contributing to the influx and the efflux, respectively. The transport model is based on work on the active uptake of morphine (Xie *et al*., 1999), simulations of different transport processes across the BBB (Hammarlund-Udenaes *et al*., 1997) and the models proposed by Upton *et al*. (2000).

To describe transport from blood-to-brain over a large concentration range, a model was developed by a stepwise approach. Linear brain distribution models with and without active efflux could not describe the data. Next, a model was developed that consisted of a perfusion (cerebral blood flow (CBF)-limited) compartment and a deeper membrane-limited compartment (the brain ECF). However, this perfusion component could not be identified nor did inclusion of this term yield a significant improvement in the goodness-of-fit. For this reason, the perfusion term was removed from the model. This indicated that CBF is not a rate-limiting step in the transport of morphine across the BBB. This was expected on the basis of its physico–chemical properties (log P ~0.7, and pK_a of 7.9) and published data on *in vivo* uptake clearance (Cl_{in}). A clearance value of 0.010 ml min^{-1} g brain was found in mice (Dagenais *et al*., 2004), and values ranging from 0.011 to 0.014 ml min^{-1} g brain in rat (Bouw *et al*., 2000; Tunblad *et al*., 2004), and an *in situ* PS value of 0.008 ml min g^{-1} brain in rat (Wu *et al*., 1997). These values are much lower than CBF values of around 1–2 ml min^{-1} g brain in mice and rats.

The non-linearity in the brain ECF concentration data indicated the presence of active efflux that was sensitive to inhibition by GF120918 as well as the presence of active saturable influx. Since, the uptake into the brain is composed of passive diffusion and active influx, the Cl_{in} is not a single value and can therefore not be directly compared with previous results. However, based on the published values of Cl_{in} ranging between 0.011 and 0.014 ml min^{-1} g brain^{-1} obtained with a rather similar experimental setting (Bouw *et al*., 2000; Tunblad *et al*., 2004), it can be concluded that this value is much smaller than rat CBF. At high doses, like many other opioids, morphine induces respiratory depression as a side effect, which results in a decrease in pO_2, an increase in pCO_2 and a decrease in pH. To keep these changes to a minimum in our experiments, artificial ventilation was applied at the 40 mg kg^{-1} dose of morphine. Passive diffusion of morphine (with pK_a of 7.9) into the brain is pH dependent and is higher at higher pH values, because relatively more uncharged morphine molecules are available. This has been demonstrated experimentally by Bouw and co-workers (2000). The artificial ventilation in our experiments prevented a decrease in pH and therefore probably has resulted in a higher value for the passive diffusion uptake clearance in our study.

The influence of an active saturable influx transporter has never been proposed in population PK analyses. In an earlier study using microdialysis in mice, the presence of an active influx process was already indicated by brain/blood ratios that were much higher at low blood concentrations, both in *mdr1a(+/+)* and *(−/−)* mice (Xie *et al*., 1999). These observations also indicated that the active influx is not sensitive to changes in Pgp efflux. Our study is the first to characterize such an active influx in quantitative terms. Other studies only had access to concentrations after a single morphine dose (1 mg kg^{-1}) with low-resolution PK microdialysis data of 30 min intervals (Letrent *et al*., 1998, 1999a) or concentrations that resulted from a dose range of 10 and 40 mg kg^{-1} that probably already had saturated the active influx component (Bouw *et al*., 2000). However, Letrent *et al*. (1999a) found morphine brain ECF/blood ratios of approximately 0.5, which were about twofold higher compared to

the brain ECF/plasma ratio of ~0.25 found by Bouw and co-workers (2000). This also supports the existence of active influx at lower blood concentrations. It remains to be elucidated, however, if such active influx is also present in and relevant for the human situation.

Several *in vitro* and *in vivo* studies have shown that morphine is a substrate for Pgp (Schinkel *et al*., 1995; Xie *et al*., 1999; Wandel *et al*., 2002; Dagenais *et al*., 2004; Letrent *et al*., 1998, 1999a, b). In this study, a clear influence of active brain efflux could also be identified, as a twofold difference in k_{eff} existed in the presence and absence of GF120918. Interestingly, the active efflux component could not be blocked completely with GF120918. The mean GF120918 blood concentration was 214 ng ml^{-1}, which was sufficient to completely block Pgp *in vivo* (personal communication from GSK) and therefore it appears that morphine efflux from the brain is also mediated by transporters other than Pgp. Tunblad and co-workers (2004) showed that morphine is also substrate for the probenecid-sensitive transporters at the BBB. Co-administration of probenecid resulted in a decrease in efflux clearance of morphine from the brain.

Apart from the Pgp inhibitor GF120918, two other drugs were co-administered with morphine in this study. First, midazolam was continuously administered to prevent opioid-induced seizure activity and second, vecuronium bromide was used for muscle relaxation to enable artificial ventilation. An important question is whether these drugs could influence Pgp functionality. For midazolam, an inhibitory effect on Pgp functionality *in vitro*, has been shown, only at high concentrations (100 μM) (Mahar Doan *et al*., 2002; Tolle-Sander *et al*., 2003). The steady-state concentrations in our experiments were around 3 μM and present in all conditions tested and therefore the influence of midazolam on Pgp could be neglected. For vecuronium bromide, we could not find any indications on a drug interaction with morphine.

In conclusion, the BBB transport of morphine could be accurately described with a model based on (slow) passive diffusion, combined with both active efflux and active saturable influx. This active efflux is partly explained by the interaction of morphine with Pgp. These observations indicate a blood concentration dependency and sensitivity to drug interactions. The complex brain distribution kinetics of morphine has an important impact for investigations on the PK/PD correlation of morphine.

Acknowledgements

We gratefully acknowledge the technical assistance of MCM Blom-Roosemalen, SM Bos-van Maastricht and P Looijmans. The supply of GF120918 by GlaxoSmithKline in the United Kingdom is highly appreciated. These investigations were financially supported by GlaxoSmithKline in the United Kingdom.

Conflict of interest

The authors state no conflict of interest.

References

Beal SL, Sheiner LB (1999). *NONMEM Users Guide*. San Francisco, CA.

Bouw MR, Gardmark M, Hammarlund-Udenaes M (2000). Pharmacokinetic-pharmacodynamic modelling of morphine transport across the blood-brain barrier as a cause of the antinociceptive effect delay in rats – a microdialysis study. *Pharm Res* **17**: 1220–1227.

Bouw MR, Hammarlund-Udenaes M (1998). Methodological aspects of the use of a calibrator in *in vivo* microdialysis-further development of the retrodialysis method. *Pharm Res* **15**: 1673–1679.

Bouw MR, Xie R, Tunblad K, Hammarlund-Udenaes M (2001). Blood–brain barrier transport and brain distribution of morphine-6-glucuronide in relation to the antinociceptive effect in rats – pharmacokinetic/pharmacodynamic modelling. *Br J Pharmacol* **134**: 1796–1804.

Bungay PM, Morrison PF, Dedrick RL (1990). Steady-state theory for quantitative microdialysis of solutes and water *in vivo* and *in vitro*. *Life Sci* **46**: 105–119.

Coughtrie MW, Ask B, Rane A, Burchell B, Hume R (1989). The enantioselective glucuronidation of morphine in rats and humans. Evidence for the involvement of more than one UDP-glucuronosyltransferase isoenzyme. *Biochem Pharmacol* **38**: 3273–3280.

Cox EH, Van Hemert JG, Tukker EJ, Danhof M (1997). Pharmacokinetic-pharmacodynamic modelling of the EEG effect of alfentanil in rats. *J Pharmacol Toxicol Methods* **38**: 99–108.

Cox EH, Veyrat-Follet C, Beal SL, Fuseau E, Kenkare S, Sheiner LB (1999). A population pharmacokinetic-pharmacodynamic analysis of repeated measures time-to-event pharmacodynamic responses: the antiemetic effect of ondansetron. *J Pharmacokinet Biopharm* **27**: 625–644.

Dagenais C, Graff CL, Pollack GM (2004). Variable modulation of opioid brain uptake by P-glycoprotein in mice. *Biochem Pharmacol* **67**: 269–276.

de Lange EC, Danhof M (2002). Considerations in the use of cerebrospinal fluid pharmacokinetics to predict brain target concentrations in the clinical setting: implications of the barriers between blood and brain. *Clin Pharmacokinet* **41**: 691–703.

Duffull SB, Aarons L (2000). Development of a sequential linked pharmacokinetic and pharmacodynamic simulation model for ivabradine in healthy volunteers. *Eur J Pharm Sci* **10**: 275–284.

Ekblom M, Gardmark M, Hammarlund-Udenaes M (1993). Pharmacokinetics and pharmacodynamics of morphine-3-glucuronide in rats and its influence on the antinociceptive effect of morphine. *Biopharm Drug Dispos* **14**: 1–11.

Gardmark M, Ekblom M, Bouw R, Hammarlund-Udenaes M (1993). Quantification of effect delay and acute tolerance development to morphine in the rat. *J Pharmacol Exp Ther* **267**: 1061–1067.

Groenendaal D, Blom-Roosemalen MC, Danhof M, Lange EC (2005). High-performance liquid chromatography of nalbuphine, butorphanol and morphine in blood and brain microdialysate samples: application to pharmacokinetic/pharmacodynamic studies in rats. *J Chromatogr B Analyt Technol Biomed Life Sci* **822**: 230–237.

Groenendaal D, Freijer J, de Mik D, Bouw MR, Danhof M, Lange EC (2007). Influence of biophase distribution and P-glycoprotein interaction on pharmacokinetic–pharmacodynamic modelling of the effects of morphine on the EEG. *Br J Pharmacol* **151**: 713–720 (this issue).

Hammarlund-Udenaes M, Paalzow LK, de Lange EC (1997). Drug equilibration across the blood–brain barrier – pharmacokinetic considerations based on the microdialysis method. *Pharm Res* **14**: 128–134.

Henthorn TK, Liu Y, Mahapatro M, Ng KY (1999). Active transport of fentanyl by the blood–brain barrier. *J Pharmacol Exp Ther* **289**: 1084–1089.

Letrent SP, Pollack GM, Brouwer KR, Brouwer KL (1998). Effect of GF120918, a potent P-glycoprotein inhibitor, on morphine pharmacokinetics and pharmacodynamics in the rat. *Pharm Res* **15**: 599–605.

Letrent SP, Pollack GM, Brouwer KR, Brouwer KL (1999a). Effects of a potent and specific P-glycoprotein inhibitor on the blood–brain barrier distribution and antinociceptive effect of morphine in the rat. *Drug Metab Dispos* **27**: 827–834.

Letrent SP, Polli JW, Humphreys JE, Pollack GM, Brouwer KR, Brouwer KL (1999b). P-glycoprotein-mediated transport of morphine in brain capillary endothelial cells. *Biochem Pharmacol* **58**: 951–957.

Mahar Doan KM, Humphreys JE, Webster LO, Wring SA, Shampine LJ, Serabjit-Singh CJ *et al*. (2002). Passive permeability and P-glycoprotein-mediated efflux differentiate central nervous system (CNS) and non-CNS marketed drugs. *J Pharmacol Exp Ther* **303**: 1029–1037.

Mandema JW, Tukker E, Danhof M (1991). Pharmacokinetic-pharmacodynamic modelling of the EEG effects of midazolam in individual rats: influence of rate and route of administration. *Br J Pharmacol* **102**: 663–668.

Moghaddam B, Bunney BS (1989). Ionic composition of microdialysis perfusing solution alters the pharmacological responsiveness and basal outflow of striatal dopamine. *J Neurochem* **53**: 652–654.

Olson RJ, Justice Jr JB (1993). Quantitative microdialysis under transient conditions. *Anal Chem* **65**: 1017–1022.

Salem A, Hope W (1997). Role of morphine glucuronide metabolites in morphine dependence in the rat. *Pharmacol Biochem Behav* **57**: 801–807.

Schinkel AH, Wagenaar E, Mol CA, van Deemter L (1996). P-glycoprotein in the blood-brain barrier of mice influences the brain penetration and pharmacological activity of many drugs. *J Clin Invest* **97**: 2517–2524.

Schinkel AH, Wagenaar E, van Deemter L, Mol CA, Borst P (1995). Absence of the mdr1a P-Glycoprotein in mice affects tissue distribution and pharmacokinetics of dexamethasone, digoxin, and cyclosporin A. *J Clin Invest* **96**: 1698–1705.

Thiebaut F, Tsuruo T, Hamada H, Gottesman MM, Pastan I, Willingham MC (1987). Cellular localization of the multidrug-resistance gene product P-glycoprotein in normal human tissues. *Proc Natl Acad Sci USA* **84**: 7735–7738.

Tolle-Sander S, Rautio J, Wring S, Polli JW, Polli JE (2003). Midazolam exhibits characteristics of a highly permeable P-glycoprotein substrate. *Pharm Res* **20**: 757–764.

Tunblad K, Jonsson EN, Hammarlund-Udenaes M (2004). Morphine blood–brain barrier transport is influenced by probenecid co-administration. *Pharm Res* **20**: 618–623.

Upton RN, Ludbrook GL, Grant C, Doolette DJ (2000). The effect of altered cerebral blood flow on the cerebral kinetics of thiopental and propofol in sheep. *Anesthesiology* **93**: 1085–1094.

van Bree JB, de Boer AG, Danhof M, Ginsel LA, Breimer DD (1988). Characterization of an '*in vitro*' blood–brain barrier: effects of molecular size and lipophilicity on cerebrovascular endothelial transport rates of drugs. *J Pharmacol Exp Ther* **247**: 1233–1239.

van Crugten JT, Somogyi AA, Nation RL, Reynolds G (1997). Concentration-effect relationships of morphine and morphine-6 beta-glucuronide in the rat. *Clin Exp Pharmacol Physiol* **24**: 359–364.

Wagner JG (1974). A safe method for rapidly achieving plasma concentration plateaus. *Clin Pharmacol Ther* **16**: 691–700.

Wandel C, Kim R, Wood M, Wood A (2002). Interaction of morphine, fentanyl, sufentanil, alfentanil, and loperamide with the efflux drug transporter P-glycoprotein. *Anesthesiology* **96**: 913–920.

Wu D, Kang YS, Bickel U, Pardridge WM (1997). Blood–brain barrier permeability to morphine-6-glucuronide is markedly reduced compared with morphine. *Drug Metab Dispos* **25**: 768–771.

Xie R, Hammarlund-Udenaes M, de Boer AG, de Lange EC (1999). The role of P-glycoprotein in blood-brain barrier transport of morphine: transcortical microdialysis studies in mdr1a (−/−) and mdr1a (+/+) mice. *Br J Pharmacol* **128**: 563–568.

Yano Y, Beal SL, Sheiner LB (2001). Evaluating pharmacokinetic/pharmacodynamic models using the posterior predictive check. *J Pharmacokinet Pharmacodyn* **28**: 171–192.